inorganics

MDPI

Article

Binding Properties of a Dinuclear Zinc(II) Salen-Type Molecular Tweezer with a Flexible Spacer in the Formation of Lewis Acid-Base Adducts with Diamines

Gabriella Munzi, Giuseppe Consiglio, Salvatore Failla and Santo Di Bella *

Dipartimento di Scienze Chimiche, Università di Catania, I-95125 Catania, Italy; gabriella.munzi@phd.unict.it (G.M.); gconsiglio@dii.unict.it (G.C.); sfailla@dii.unict.it (S.F.)
* Correspondence: sdibella@unict.it

Abstract: In this paper we report the binding properties, by combined ^{1}H NMR, optical absorption, and fluorescence studies, of a molecular tweezer composed of two Zn(salen)-type Schiff-base units connected by a flexible spacer, towards a series of ditopic diamines having a strong Lewis basicity, with different chain length and rigidity. Except for the 1,2-diaminoethane, in all other cases the formation of stable 1:1 Lewis acid-base adducts with large binding constants is demonstrated. For α,ω-aliphatic diamines, binding constants progressively increase with the increasing length of the alkyl chain, thanks to the flexible nature of the spacer and the parallel decreased conformational strain upon binding. Stable adducts are also found even for short diamines with rigid molecular structures. Given their preorganized structure, these latter species are not subjected to loss of degrees of freedom. The binding characteristics of the tweezer have been exploited for the colorimetric and fluorometric selective and sensitive detection of piperazine.

Keywords: zinc(II) complexes; Schiff-bases; molecular tweezers; Lewis acid-base adducts

Citation: Munzi, G.; Consiglio, G.; Failla, S.; Di Bella, S. Binding Properties of a Dinuclear Zinc(II) Salen-Type Molecular Tweezer with a Flexible Spacer in the Formation of Lewis Acid-Base Adducts with Diamines. *Inorganics* **2021**, *9*, 49. https://doi.org/10.3390/inorganics9060049

Academic Editor: Isabel Correia

Received: 27 April 2021
Accepted: 11 June 2021
Published: 16 June 2021

1. Introduction

"Molecular tweezers" refer to bifunctional molecular receptors characterized by the presence of two binding sites connected with a more or less rigid spacer [1,2]. They have the ability to form complexes with a substrate molecule, resembling a tweezer holding an object. Depending on the nature of the binding sites and on the conformational rigidity of the spacer, they find various applications such as in molecular recognition [1,3], including biomolecules [4–6], or fullerenes [7], enzyme inhibition or prevention of protein aggregation [8–10], catalysis [11], switchable molecular tweezers [12,13], electrochemical switches [14,15], and as building blocks for supramolecular nanostructures [16,17].

Various molecular tweezers have been synthesized as hosts for guest molecules. Among them, glycoluril- [1,2] or porphyrin-based [3] tweezers are those most studied. The latter have been involved in various investigations for their ability to bind ditopic species, e.g., for configuration [18,19] and chirogenesis [20–23] studies, and for the development of sensors targeting specific molecules [24], including chiral species [25,26]. Moreover, the binding behavior with ditopic guests of different length and rigidities has also been explored [27–30].

Zn(salen)-type Schiff-base complexes have recently been investigated for their sensing properties [31–33], mostly related to their Lewis acidic character [34]. These complexes easily coordinate Lewis bases with formation of Lewis acid-base adducts, and this process is accompanied by relevant changes of their spectroscopic properties. Among them, derivatives from the 2,3-diaminomaleonitrile, Zn(salmal) [35,36], are those mostly studied for sensing a variety of Lewis bases [37–44].

Recently, a dinuclear Zn(salmal) Schiff-base complex (**1**, Scheme 1) whose units are connected with a non-conjugated, flexible spacer, has been synthesized and characterized [45].

It has been found that in non-coordinating solvents **1** is stabilized by the formation of intramolecular aggregates, which hardly deaggregate by addition of monotopic Lewis bases. However, in the presence of strong ditopic Lewis bases, such as diamines, the complex easily deaggregates with formation of 1:1 adducts, thus acting as a "molecular tweezer". Deaggregation is accompanied by relevant optical absorption changes and a substantial enhancement of the fluorescence. Therefore, **1** has been investigated for the selective and sensitive detection of some biogenic diamines [46].

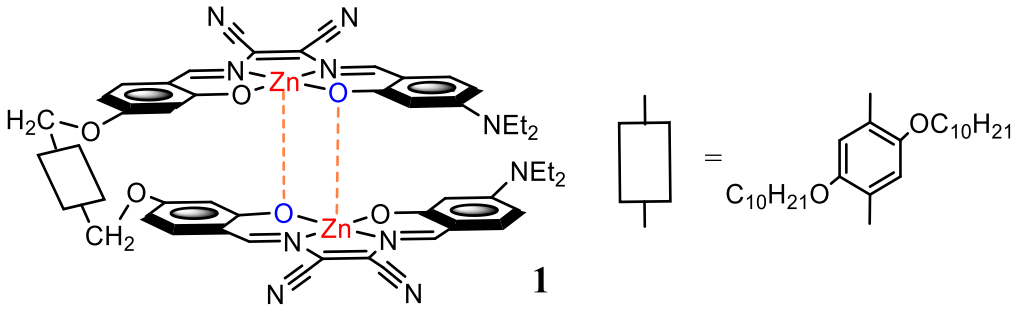

Scheme 1. Structure of the dinuclear complex **1**.

As the dinuclear aggregate complex **1** acts as a "molecular tweezer" upon deaggregation, this is an unusual feature compared to conventional tweezers characterized by binding sites kept separate by a spacer. Thus, starting from the defined aggregate **1**, in the formation of Lewis acid-base adducts, it will not be subjected to binding as a consequence of a specific conformation of the Lewis base. Rather, the ability of the Lewis base to bind the aggregate could be related to its basicity and to the stability of the adduct. It is thus interesting to investigate the features affecting the binding interactions between the aggregate molecular tweezer **1**, having a flexible spacer, and the structure of the ditopic Lewis bases.

The aim of this work is to study, through ^{1}H NMR, UV/vis, and fluorescence spectroscopies, the binding interactions of the tweezer **1** with diamines of different chain length and rigidity, to better understand their Lewis acid-base interactions.

2. Results and Discussion

To study the binding of various diamines to the molecular tweezer **1**, either aliphatic, alicyclic, and aromatic diamines were considered (Scheme 2). In particular, the flexible primary α,ω-aliphatic diamines, $NH_2(CH_2)_nNH_2$ (n = 2–12), were studied, and the results compared with those related to the rigid diamines, piperazine (PZ), 1,4-diazabicyclo[2.2.2]octane (DABCO), and 4,4′-bipyridine (BPY), and the semi-rigid 1,2-bis(4-pyridyl)ethane (DPE).

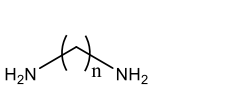

n = 2; 1,2-Diaminoethane
n = 3; 1,3-Diaminopropane
n = 4; 1,4-Diaminobutane
n = 5; 1,5-Diaminopentane
n = 6; 1,6-Diaminohexane
n = 8; 1,8-Diaminooctane
n = 10; 1,10-Diaminodecane
n = 12; 1,12-Diaminododecane

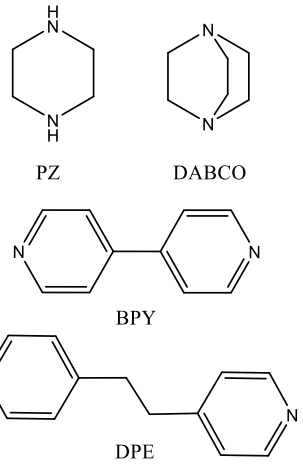

Scheme 2. Structure of investigated diamines.

UV/vis optical absorption and fluorescence spectral data and binding constants for the formation of (1:1) **1**·diamine adducts (equilibrium (1)) are reported in Table 1. Spectrophotometric and spectrofluorometric titrations for the representative 1,10-diaminodecane are reported in Figures 1 and 2.

$$\mathbf{1}\ (\text{soln}) + \text{diamine}\ (\text{soln}) \rightleftharpoons \mathbf{1}\ \text{diamine}\ (\text{soln}) \quad (1)$$

In all instances, the binding of diamines to **1** involves an increase of the optical absorption band centered at λ_{max} = 580 nm and an enhancement of fluorescence intensity at $\lambda_{max} \cong$ 614 nm (e.g., the fluorescence quantum yield, ϕ, increases from 0.03 to 0.29 on switching from **1** to the adduct with 1,10-diaminodecane). Moreover, with the exception of diaminoethane, optical absorption spectra show the presence of multiple isosbestic points, indicative of the formation of species with a defined stoichiometry. Job's plot analyses clearly indicate the formation of 1:1 adducts.

Table 1. Binding constants and optical spectroscopic data for investigated **1**·diamine adducts [a] in chloroform solution.

Diamine	log K	Absorption λ_{max} (nm)	Emission λ_{max} (nm)
1		582	625
PZ	5.4 ± 0.1	580	618
DABCO	5.6 ± 0.2	580	614
DPE	4.0 ± 0.1	579	614
BPY	2.1 ± 0.2 (K_1) 3.6 ± 0.2 (K_2)	580	611
1,2-Diaminoethane	-	583	614
1,3-Diaminopropane	2.9 ± 0.1	580	614
1,4-Diaminobutane [b]	4.3 ± 0.1	580	618
1,5-Diaminopentane [b]	5.0 ± 0.2	580	618
1,6-Diaminohexane	5.1 ± 0.1	580	614
1,8-Diaminooctane	6.4 ± 0.1	587	616
1,10-Diaminodecane	6.2 ± 0.2	580	614
1,12-Diaminododecane	5.9 ± 0.2	580	614

[a] For comparison, **1**·(pyridine)$_2$; λ_{max} = 579 nm (absorption); λ_{max} = 613 nm (emission); log K_1 = 2.35; log K_2 = 3.58; from ref. [45]. [b] from ref. [46].

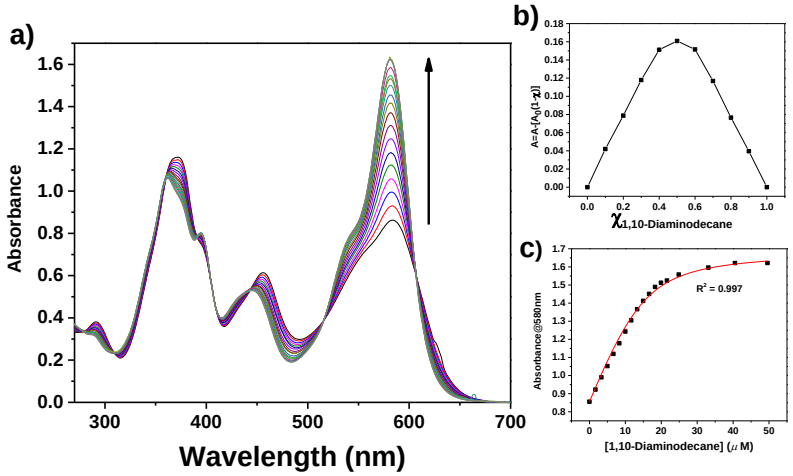

Figure 1. (**a**) Optical absorption titration curves of **1** (15 μM solution in $CHCl_3$) with addition of 1,10-diaminodecane. The concentration of 1,10-diaminodecane added varied from 0 to 50 μM. (**b**) Job's plot for the binding of **1** with 1,10-diaminodecane. The total concentration of **1** and 1,10-diaminodecane is 15 μM. (**c**) Variation of the absorbance at 580 nm as a function of the concentration of 1,10-diaminodecane added and fit of the binding isotherm with Equation (1) (red line).

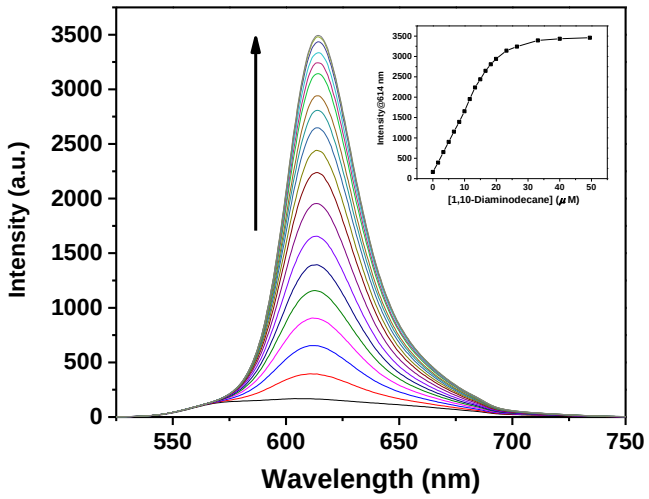

Figure 2. Fluorescence titration curves of **1** (15 μM solution in $CHCl_3$; λ_{exc} = 516 nm) with addition of 1,10-diaminodecane. The concentration of 1,10-diaminodecane added varied from 0 to 50 μM. Inset: variation of the fluorescence intensity at 614 nm as a function of the concentration of 1,10-diaminodecane added.

2.1. α,ω-Aliphatic Diamines

As is shown in Table 1, a substantial variation of the binding constants with the chain length is observed. Despite the analogous Lewis basicity [47] along this investigated series of aliphatic, linear primary diamines, binding constants span over more than three orders of magnitude. While shorter diamines are characterized by relatively low binding constants, the increasing of the chain length parallels an increase of binding constant values. Largest binding constants are reached with the 1,8-diaminooctane, and then remain almost unchanged, even if slightly smaller, on further increase of the chain length.

^{1}H NMR titration studies further support the formation of 1:1 adducts. The titration for the representative 1,10-diaminodecane is reported in Figure 3. In particular, after the addition of half stoichiometric amount of 1,10-diaminodecane to a $CDCl_3$ solution of **1**, the ^{1}H NMR spectrum shows some changes with the appearance of new broad signals. A complete variation of the ^{1}H NMR spectrum, with the presence of broad signals, is observed after the addition of a stoichiometric amount of 1,10-diaminodecane. Finally, upon the addition of 4-fold molar excess of 1,10-diaminodecane the spectrum evolves towards a set of sharp signals, except for the down-field shifted H_3 and H_3' protons which remain slightly broad, indicative of the formation of a defined 1:1: adduct. Moreover, the doublet of doublet benzylic proton signals, H_5, of the aggregate complex **1** becomes a sharp singlet, indicating that the restricted rotation around the benzylic bonds is no longer operating in the adduct.

1,2-Diaminoethane behaves quite differently. In fact, starting from 10 μM solutions of **1** a detectable variation of optical absorption or fluorescence spectra occurs after the addition of ca. 2-fold molar excess of diaminoethane, while the saturation point is reached by the addition of ca. 800-fold molar excess, unlike longer diamines which form 1:1 adducts with **1** by addition of stoichiometric amounts. Moreover, in contrast with longer diamines, optical absorption spectra do not show any isosbestic point. These observations suggest the formation of multiple, instead of single, adducts (e.g., 1:2 adducts), likely favored by the presence of the large stoichiometric excess of diamine.

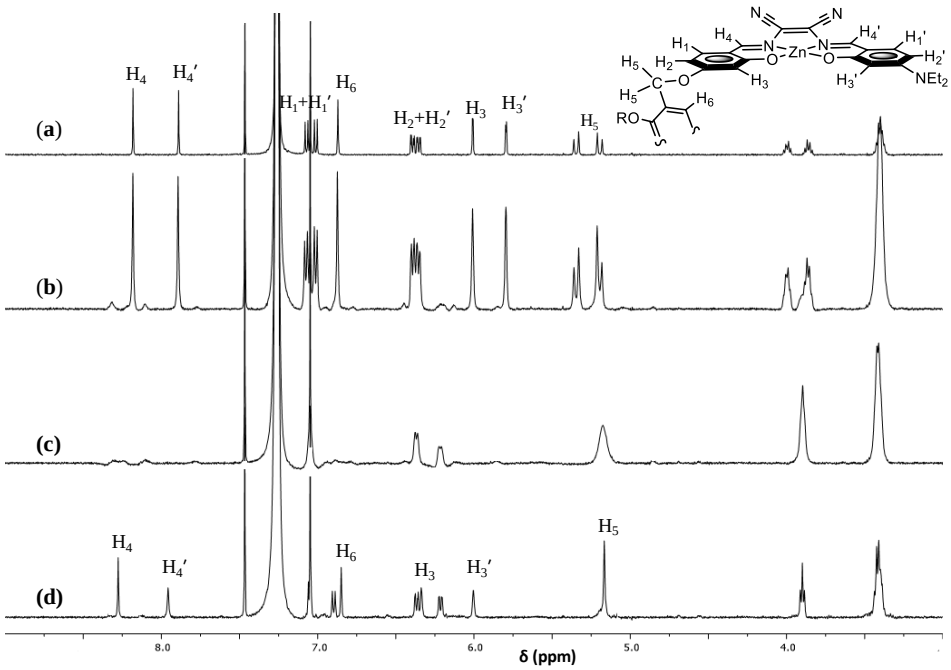

Figure 3. ^{1}H NMR titration spectra of **1** (50 μM in $CDCl_3$ (**a**)) with addition of 1,10-diaminodecane. The concentration of 1,10-diaminodecane added was 25 μM (**b**), 50 μM (**c**), and 200 μM (**d**). For assignment of ^{1}H NMR signals of the aggregate **1**. Adapted from ref. [45].

As binding constants for the formation of **1**·diamine adducts reflect the relative stability of the adducts with respect to the aggregate [48], given the analogous Lewis basicity along the series of diamines and the entropic cost upon binding the diamine to **1**, the increasing binding constants with the increased length of diamines can be related to an increased stability of the intramolecular cyclic adducts. In view of the flexibility of the spacer in the tweezer **1**, which in principle can accommodate almost any ditopic Lewis base, the different binding constants along the series could be attributed to a larger entropic cost of the loss of degrees of freedom for diamines with a shorter alkyl chain, while the involved longer α,ω-diamines are not subjected to conformational strain upon binding, resulting in larger intramolecular cyclic adducts, also with gain of degrees of freedom of the flexible spacer of the tweezer.

In comparison to host–guest studies involving glycoluril- or porphyrin-based tweezers with ditopic guests of different length, **1** behaves quite differently, being characterized by increasing binding constants with increasing chain length of diamines. In fact, it has been found that most of these investigated tweezers, having rigid or semi-flexible spacers, show a preference for a particular guest, rather than for shorter or longer ones. This has been associated with the guest best matching the distance between the binding sites of the tweezer [27–30,49–51].

2.2. Rigid Diamines

The binding interaction for the formation of **1**·diamine adducts is also affected by the rigidity of the diamine. PZ is a cyclic secondary diamine with a N-N distance comparable to that of 1,2-diaminoethane. In spite of this, PZ forms stable 1:1 adducts with **1**, with a large binding constant (Table 1), especially if compared to that of aliphatic diamines with shorter chain length ($n \leq 4$). DABCO is a bicyclic tertiary diamine whose N-N distance is comparable to that of PZ. It has been widely used to study the binding characteristics of porphyrin-based tweezers [22,30,52–54]. Again, DABCO binds easily with **1** with a binding constant slightly higher than that of PZ. This is consistent with the greater Lewis basicity of the tertiary alicyclic DABCO with respect to the secondary alicyclic PZ [47].

It therefore turns out that the preorganized structure of PZ and DABCO favors the formation of stable adducts because, except for the entropic cost upon binding the diamine to **1**, these species are not subjected to loss of degrees of freedom, contrary to aliphatic diamines with short alkyl chain.

^{1}H NMR titrations using DABCO as titrant suggest the formation of stable 1:1 adducts even for alicyclic diamines (Figure 4). In this case, however, when half stoichiometric amount of DABCO is added to $CDCl_3$ solution of **1**, two sets of signals are evident in the spectrum. This indicates the presence in solution of the aggregate complex **1** and its adduct with DABCO, in a slow equilibrium on the NMR time scale. Moreover, from the comparison of the signal of H_5 protons, a sharper singlet is observed for the adduct with 1,10-diaminodecane, with respect to the broad signal for that with DABCO. This suggests a greater mobility of benzyl hydrogens in the larger intramolecular cyclic **1**·diaminodecane adduct compared to those of the **1**·DABCO adduct (Figure 5).

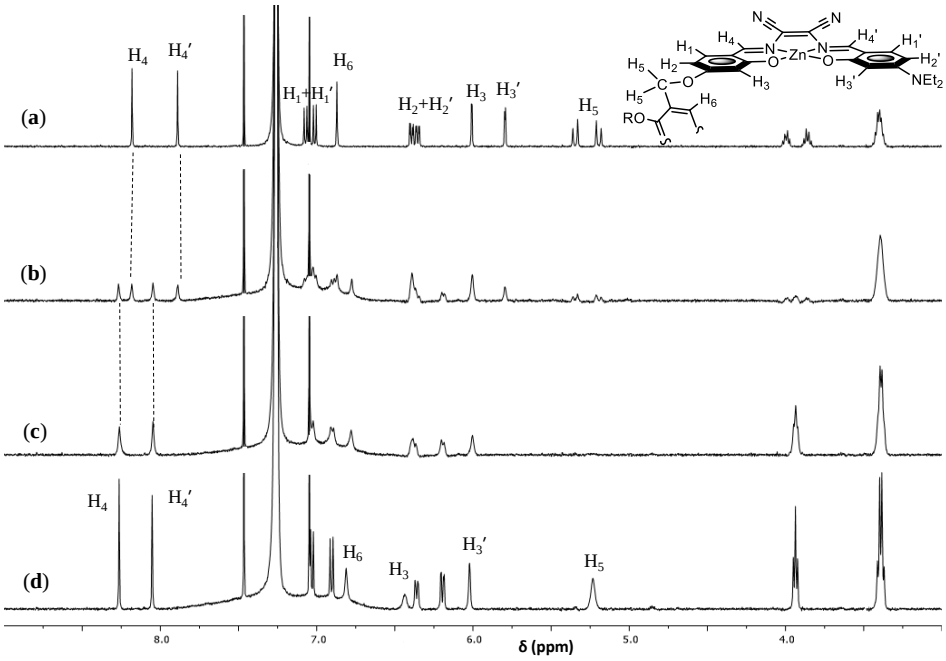

Figure 4. ^{1}H NMR titration spectra of **1** (50 μM in $CDCl_3$ (**a**)) with addition of DABCO. The concentration of DABCO added was 25 μM (**b**), 100 μM (**c**), and 200 μM (**d**).

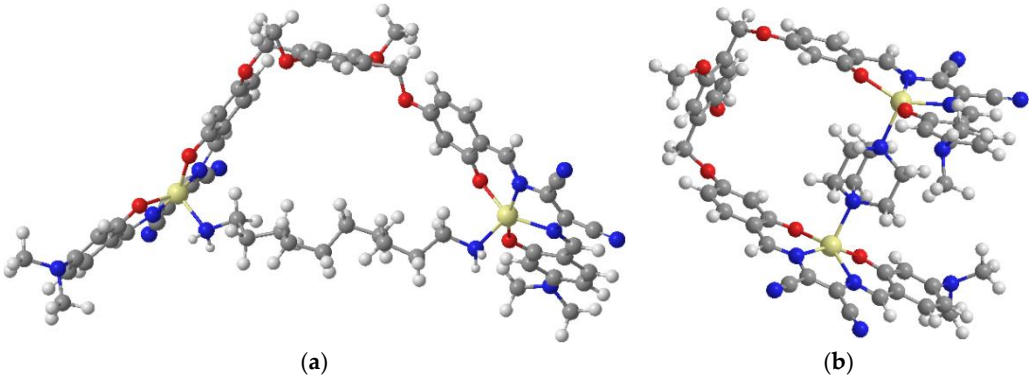

Figure 5. (**a**) Modeling (PM3, using the HyperChem Software (8.0)) of the **1**·diaminodecane adduct and (**b**) modeling of the 1·DABCO adduct.

The structure of DPE is more rigid than that of *α*,*ω*-aliphatic diamines because of the presence of two heterocyclic aromatic rings linked by an ethyl group. In the *anti*-conformation, a N-N distance of 9.3 Å can be estimated, slightly longer than that

of 1,6-diaminohexane (8.7 Å). However, the binding constant of DPE results are one order of magnitude lower than that of 1,6-diaminohexane. This can be attributed to a higher conformational strain upon binding DPE to **1**, in comparison with the flexible diaminohexane.

BPY was also investigated as rigid diamine. Spectrophotometric titrations again indicate the formation of a defined species; by the presence of multiple isosbestic points, however, the saturation point is reached with ca. a 500-fold molar excess of BPY. In this case the binding isotherm is fitted with a model involving a 1:2 adduct (equilibria (2)), instead of a 1:1 adduct (equilibrium (1)).

$$\mathbf{1}\ (\text{soln}) + \text{BPY}\ (\text{soln}) \rightleftharpoons \mathbf{1}\cdot\text{BPY} \quad (2)$$

$$\mathbf{1}\cdot\text{BPY}\ (\text{soln}) + \text{BPY}\ (\text{soln}) \rightleftharpoons \mathbf{1}\cdot(\text{BPY})_2\ (\text{soln}) \quad (2')$$

Even if the ditopic BPY is expected to possess a strong Lewis basicity comparable to pyridine, it behaves as a monotopic species. Deaggregation of **1** with pyridine gave the same results (Table 1) [45].

2.3. Sensing Piperazine

The molecular tweezer **1** can be used as a suitable chemodosimeter for the detection of piperazine. PZ possesses important pharmacological properties and is used, together with its salts, as an anthelmintic [55], in industrial gas treatments such as CO_2 capture system [56,57], and also as the precursor for a class of psychogenic drugs [58,59]. Piperazine may cause allergic dermatitis [60], and it has been demonstrated that, although not extremely toxic, it has a low biodegradability [61]. Detection of PZ is thus relevant for environment monitoring and protection [62].

The tweezer **1** allows both the colorimetric and fluorometric selective and sensitive detection of PZ. A calculated limit of detection (LOD) down to 0.76 μM and 0.33 μM is obtained from the spectrophotometric and spectrofluorometric data, respectively, with a linear dynamic range up to 10 μM (Figures 6 and 7). These values are better than those reported in the literature using spectrophotometric methods [63–66]. Various other techniques have been developed for the detection and quantitation of piperazine, such as HPLC [67], voltammetry [68], or capillary electrophoresis [69]; most of them, however, require time-consuming procedures. Therefore, the development of simple and direct methods for sensing piperazine is highly desirable. In this regard, only a few optical chemosensors are reported in the literature for the selective detection of PZ [70–72].

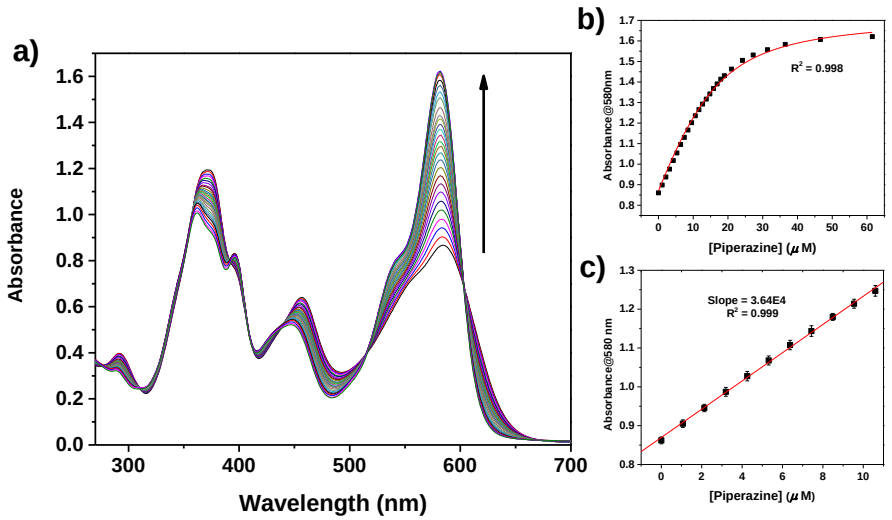

Figure 6. (**a**) Optical absorption titration curves of **1** (15 μM solution in $CHCl_3$) with addition of PZ. The concentration of PZ added varied from 0 to 60 μM. (**b**) Variation of the absorbance at 580 nm as a function of the concentration of PZ added and fit of the binding isotherm with Equation (1) (red line). (**c**) Linear best fit in the linear dynamic range (weight given by data error bars).

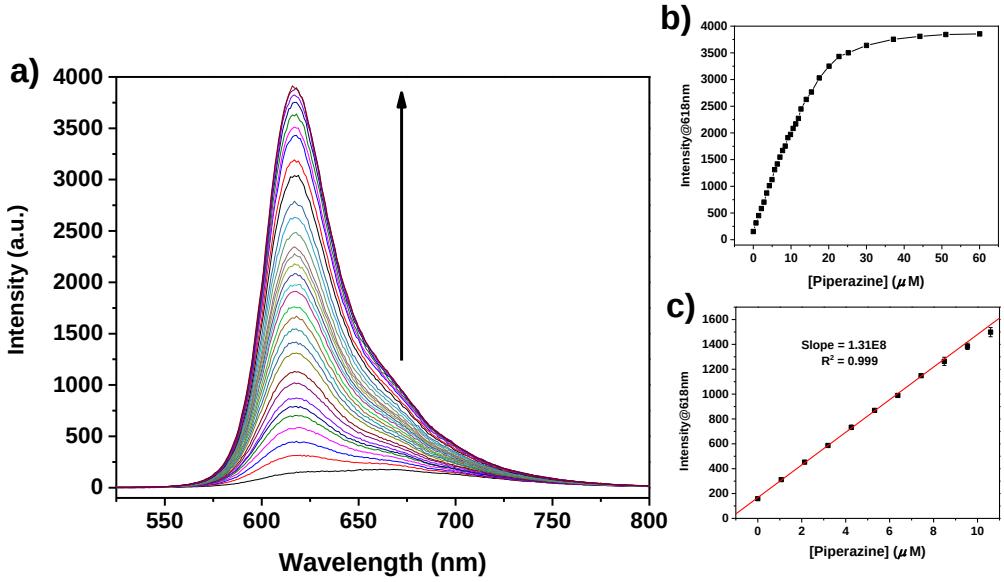

Figure 7. (**a**) Fluorescence titration curves of **1** (15 μM solution in $CHCl_3$; λ_{exc} = 515 nm) with addition of PZ. The concentration of PZ added varied from 0 to 60 μM. (**b**) Variation of the fluorescence intensity at 618 nm as a function of the concentration of PZ added. (**c**) Linear best fit in the linear dynamic range (weight given by data error bars).

The selectivity of **1** towards PZ was proven by performing competitive experiments. These were conducted by mixing a solution of **1** with PZ (1:1 molar ratio) and a 10-fold molar excess of interferent (Figure 8). These results were then compared with those obtained by adding to **1** either PZ in an equimolar amount, or the interferent in a 10-fold molar excess. As potential interferents, some monotopic species with a strong Lewis basicity were considered. Pyridine was chosen as the heterocyclic aromatic amine, while isopropylamine, diethylamine, and triethylamine were chosen as prototype compounds of primary, secondary, and tertiary amines. Moreover, the heteroditopic 4-amino-1-butanol, bearing two different coordinating sites with a different Lewis basicity, was also considered. As shown in Figure 8, very small or no changes of the absorbance at λ_{max} = 580 nm are observed after the addition of each potential interferent, especially for diethylamine and triethylamine. Therefore, these data suggest that **1** can be considered a selective receptor towards PZ, even in the presence of common aliphatic or aromatic monotopic or heteroditopic amines.

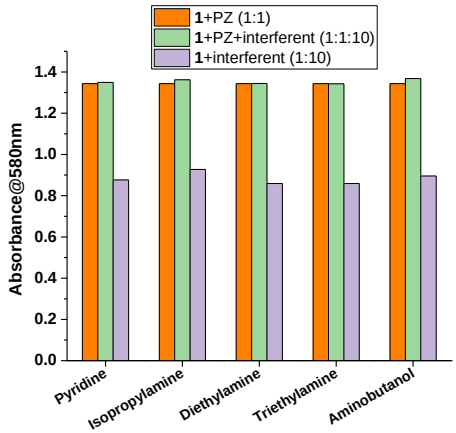

Figure 8. Absorbance of **1** at 580 nm upon the addition of an equimolar amount (15 μM) of piperazine (orange bars); upon the addition of an equimolar amount (15 μM) of piperazine with the presence of 10-fold molar excess (150 μM) of interferent (green bars); upon the addition of 10-fold molar excess (150 μM) of interferent (violet bars).

3. Experimental Section

3.1. Materials and General Procedures

All the chemicals used were purchased from Sigma-Aldrich (Darmstadt, Germany) and used as received. Complex **1** was synthesized and purified as previously reported [45]. Chloroform stabilized with amylene was used for optical absorption and fluorescence titrations. Before being used, it was purified as follows: dried on anhydrous K_2CO_3 for 2 h, filtered and stored over molecular sieves (3 Å) in the dark under argon atmosphere. Chloroform solutions of **1** were prepared by dissolving the compound in chloroform and filtering it through a 0.2 μm Teflon membrane filter. $CDCl_3$ was stored over molecular sieves (3 Å).

3.2. Physical Measurements

^{1}H NMR measurements were run at 27 °C on a Varian Unity S 500 (499.88 MHz for ^{1}H) spectrometer. Tetramethylsilane was used as internal reference for all NMR experiments. Optical absorption spectra were recorded at room temperature with an Agilent Cary 60 spectrophotometer. Fluorescence spectra were recorded at room temperature using a JASCO FP-8200 spectrofluorometer (JASCO Europe). Spectrophotometric and fluorometric titrations were performed with a 1 cm path cell using 15 μM chloroform solutions of **1**. Chloroform solutions of involved Lewis bases were added to the solution of **1** using Rainin (METTLER TOLEDO, Columbus, OH, USA) positive displacements pipettes. At least three replicate titrations were performed for each diamine. In fluorometric titrations, the wavelength of excitation was chosen in an isosbestic point. The fluorescence quantum yield was obtained using fluorescein (ϕ_F = 0.925) in 0.1 M NaOH as a standard. The absorbance value of the samples at and above the excitation wavelength was lower than 0.1 for 1 cm path length cuvettes.

3.3. Calculation of Binding Constants and Limit of Detection

Binding constants, K, for the formation of **1** diamine adducts (equilibrium 1) were calculated by fitting the binding isotherms, obtained from the plot of A vs. c_A from spectrophotometric titration data, with Equation (1) [73,74].

$$A = A_0 + \frac{A_{lim} - A_0}{2c_0}\left[c_0 + c_{DA} + 1/K - \left[(c_0 + c_{DA} + 1/K)^2 - 4c_0c_{DA}\right]^{1/2}\right]. \quad (1)$$

where A_0 is the initial absorbance of the solution having a concentration c_0, A is the absorbance intensity after addition of a given amount of diamine (DA) at a concentration c_{DA}, and A_{lim} is the limiting absorbance reached in the presence of an excess of DA. Further details are reported elsewhere [46,48]. These calculated binding constants are comparable to those previously obtained by a multivariate analysis from spectrophotometric titrations of **1** with PZ, DPE, and 1,4-diaminobutane [45]. In the case of BPY, binding constants K_1 and K_2 for a 1:2 adduct (equilibria (2)) were calculated by fitting the binding isotherm using Equation (35) of Ref. [73].

The limit of detection (LOD) was estimated, both from optical absorption or fluorescence data, according to IUPAC recommendations (Equation (2)) [75,76].

$$LOD = K \times S_b/S \quad (2)$$

where K = 3, S_b is the standard deviation of the blank solution, i.e., the absorbance or fluorescence signal of **1**, and S is the slope of the calibration curve obtained from the plot of the absorbance or fluorescence intensity of **1** vs. the concentration of the DA added. Each point is related to the mean value obtained from at least three replicate measurements. Twenty blank replicates were considered.

4. Conclusions

The binding properties of a molecular tweezer, composed of two Zn(salmal) units connected by a flexible spacer, towards a series of ditopic diamines having strong Lewis basicity have been explored by means of combined ^{1}H NMR, optical absorption, and fluorescence studies. The formation of stable 1:1 Lewis acid-base adducts with large binding constants is demonstrated. For α,ω-aliphatic diamines, binding constants progressively increase with the increasing length of the alkyl chain, thanks to the flexible nature of the spacer and there is a parallel decrease of the conformational strain upon binding for longer diamines, reaching the largest value for the 1,8-diaminooctane. Stable adducts are also found even for short diamines with rigid molecular structures. The preorganized structure of these ditopic species which, except for the entropic cost upon binding the diamine to **1**, are not subjected to loss of degrees of freedom, accounts for the large binding constants.

These binding characteristics can be exploited for the detection of ditopic strong Lewis bases. The colorimetric and fluorometric selective and sensitive detection has been demonstrated for piperazine.

Author Contributions: All experimental work was performed by G.M., G.C. and S.F. Data analysis was performed by G.M., S.F. and S.D.B. The manuscript was written by S.D.B., with contributions from the other authors. All authors have read and agreed to the published version of the manuscript.

Funding: This research received no external funding.

Institutional Review Board Statement: Not applicable.

Informed Consent Statement: Not applicable.

Data Availability Statement: Not Applicable.

Acknowledgments: This work was supported by the University of Catania, PIACERI 2020/2022, Linea di Intervento 2.

Conflicts of Interest: The authors declare no conflict of interest.

References

1. Hardouin–Lerouge, M.; Hudhomme, P.; Sallé, M. Molecular clips and tweezers hosting neutral guests. *Chem. Soc. Rev.* **2011**, *40*, 30–43. [CrossRef]
2. Leblond, J.; Petitjean, A. Molecular Tweezers: Concepts and Applications. *ChemPhysChem* **2011**, *12*, 1043–1051. [CrossRef]
3. Valderrey, V.; Aragay, G.; Ballester, P. Porphyrin tweezer receptors: Binding studies, conformational properties and applications. *Co-Ord. Chem. Rev.* **2014**, *258-259*, 137–156. [CrossRef]
4. Klärner, F.-G.; Schrader, T. Aromatic Interactions by Molecular Tweezers and Clips in Chemical and Biological Systems. *Acc. Chem. Res.* **2012**, *46*, 967–978. [CrossRef] [PubMed]
5. Gong, X.; Zhou, W.; Li, D.; Chai, Y.; Xiang, Y.; Yuan, R. RNA-regulated molecular tweezers for sensitive fluorescent detection of microRNA from cancer cells. *Biosens. Bioelectron.* **2015**, *71*, 98–102. [CrossRef]
6. Fokkens, M.; Schrader, T.; Klärner, F.-G. A Molecular Tweezer for Lysine and Arginine. *J. Am. Chem. Soc.* **2005**, *127*, 14415–14421. [CrossRef] [PubMed]
7. Pérez, E.M.; Martín, N. Molecular tweezers for fullerenes. *Pure Appl. Chem.* **2010**, *82*, 523–533. [CrossRef]
8. Mbarek, A.; Moussa, G.; Chain, J.L. Pharmaceutical Applications of Molecular Tweezers, Clefts and Clips. *Molecules* **2019**, *24*, 1803. [CrossRef]
9. Hadrovic, I.; Rebmann, P.; Klärner, F.-G.; Bitan, G.; Schrader, T. Molecular Lysine Tweezers Counteract Aberrant Protein Aggregation. *Front. Chem.* **2019**, *7*, 657. [CrossRef]
10. Schrader, T.; Bitan, G.; Klärner, F.-G. Molecular tweezers for lysine and arginine—Powerful inhibitors of pathologic protein aggregation. *Chem. Commun.* **2016**, *52*, 11318–11334. [CrossRef]
11. Gianneschi, N.C.; Cho, S.-H.; Nguyen, S.; Mirkin, C.A. Reversibly Addressing an Allosteric Catalyst In Situ: Catalytic Molecular Tweezers. *Angew. Chem. Int. Ed.* **2004**, *43*, 5503–5507. [CrossRef]
12. Doistau, B.; Benda, L.; Cantin, J.-L.; Cador, O.; Pointillart, F.; Wernsdorfer, W.; Chamoreau, L.-M.; Marvaud, V.; Hasenknopf, B.; Vives, G. Dual switchable molecular tweezers incorporating anisotropic Mn^{III}–salphen complexes. *Dalton Trans.* **2020**, *49*, 8872–8882. [CrossRef]
13. Doistau, B.; Tron, A.; Denisov, S.A.; Jonusauskas, G.; McClenaghan, N.D.; Gontard, G.; Marvaud, V.; Hasenknopf, B.; Vives, G. Terpy(Pt-salphen)$_2$ Switchable Luminescent Molecular Tweezers. *Chem. A Eur. J.* **2014**, *20*, 15799–15807. [CrossRef]

14. Doistau, B.; Benda, L.; Cantin, J.-L.; Chamoreau, L.-M.; Ruiz, E.; Marvaud, V.; Hasenknopf, B.; Vives, G. Six States Switching of Redox-Active Molecular Tweezers by Three Orthogonal Stimuli. *J. Am. Chem. Soc.* **2017**, *139*, 9213–9220. [CrossRef]
15. Krykun, S.; Dekhtiarenko, M.; Canevet, D.; Carré, V.; Aubriet, F.; Levillain, E.; Allain, M.; Voitenko, Z.; Sallé, M.; Goeb, S. Metalla-Assembled Electron-Rich Tweezers: Redox-Controlled Guest Release Through Supramolecular Dimerization. *Angew. Chem. Int. Ed.* **2020**, *59*, 716–720. [CrossRef] [PubMed]
16. Gao, Z.; Han, Y.; Gao, Z.; Wang, F. Multicomponent Assembled Systems Based on Platinum(II) Terpyridine Complexes. *Acc. Chem. Res.* **2018**, *51*, 2719–2729. [CrossRef]
17. Han, Y.; Tian, Y.; Li, Z.; Wang, F. Donor–acceptor-type supramolecular polymers on the basis of preorganized molecular tweezers/guest complexation. *Chem. Soc. Rev.* **2018**, *47*, 5165–5176. [CrossRef] [PubMed]
18. Li, X.; Tanasova, M.; Vasileiou, C.; Borhan, B. Fluorinated Porphyrin Tweezer: A Powerful Reporter of Absolute Configuration for erythro and threo Diols, Amino Alcohols, and Diamines. *J. Am. Chem. Soc.* **2008**, *130*, 1885–1893. [CrossRef]
19. Huang, X.; Rickman, B.H.; Borhan, B.; Berova, N.; Nakanishi, K. Zinc Porphyrin Tweezer in Host−Guest Complexation: Determination of Absolute Configurations of Diamines, Amino Acids, and Amino Alcohols by Circular Dichroism. *J. Am. Chem. Soc.* **1998**, *120*, 6185–6186. [CrossRef]
20. Borovkov, V.V.; Lintuluoto, J.M.; Hembury, G.A.; Sugiura, M.; Arakawa, R.; Inoue, Y. Supramolecular Chirogenesis in Zinc Porphyrins: Interaction with Bidentate Ligands, Formation of Tweezer Structures, and the Origin of Enhanced Optical Activity. *J. Org. Chem.* **2003**, *68*, 7176–7192. [CrossRef]
21. Brahma, S.; Ikbal, S.A.; Rath, S.P. Synthesis, Structure, and Properties of a Series of Chiral Tweezer–Diamine Complexes Consisting of an Achiral Zinc(II) Bisporphyrin Host and Chiral Diamine Guest: Induction and Rationalization of Supramolecular Chirality. *Inorg. Chem.* **2014**, *53*, 49–62. [CrossRef] [PubMed]
22. Blom, M.; Norrehed, S.; Andersson, C.-H.; Huang, H.; Light, M.E.; Bergquist, J.; Grennberg, H.; Gogoll, A. Synthesis and Properties of Bis-Porphyrin Molecular Tweezers: Effects of Spacer Flexibility on Binding and Supramolecular Chirogenesis. *Molecules* **2015**, *21*, 16. [CrossRef] [PubMed]
23. Norrehed, S.; Johansson, H.; Grennberg, H.; Gogoll, A. Improved Stereochemical Analysis of Conformationally Flexible Diamines by Binding to a Bisporphyrin Molecular Clip. *Chem. A Eur. J.* **2013**, *19*, 14631–14638. [CrossRef]
24. Lubian, E.; Baldini, F.; Giannetti, A.; Trono, C.; Carofiglio, T. Solid-supported Zn(II) porphyrin tweezers as optical sensors for diamines. *Chem. Commun.* **2010**, *46*, 3678–3680. [CrossRef]
25. Li, X.; Burrell, C.E.; Staples, R.J.; Borhan, B. Absolute Configuration for 1,*n*-Glycols: A Nonempirical Approach to Long-Range Stereochemical Determination. *J. Am. Chem. Soc.* **2012**, *134*, 9026–9029. [CrossRef]
26. Li, X.; Borhan, B. Prompt Determination of Absolute Configuration for Epoxy Alcohols via Exciton Chirality Protocol. *J. Am. Chem. Soc.* **2008**, *130*, 16126–16127. [CrossRef]
27. Crossley, M.J.; Hambley, T.W.; Mackay, L.G.; Try, A.C.; Walton, R. Porphyrin analogues of Tröger's base: Large chiral cavities with a bimetallic binding site. *J. Chem. Soc. Chem. Commun.* **1995**, 1077–1079. [CrossRef]
28. Hayashi, T.; Nonoguchi, M.; Aya, T.; Ogoshi, H. Molecular recognition of α,ω-diamines by metalloporphyrin dimer. *Tetrahedron Lett.* **1997**, *38*, 1603–1606. [CrossRef]
29. Carofiglio, T.; Lubian, E.; Menegazzo, I.; Saielli, G.; Varotto, A. Melamine-Bridged Bis(porphyrin-ZnII) Receptors: Molecular Recognition Properties. *J. Org. Chem.* **2009**, *74*, 9034–9043. [CrossRef]
30. Norrehed, S.; Polavarapu, P.; Yang, W.; Gogoll, A.; Grennberg, H. Conformational restriction of flexible molecules in solution by a semirigid bis-porphyrin molecular tweezer. *Tetrahedron* **2013**, *69*, 7131–7138. [CrossRef]
31. Consiglio, G.; Oliveri, I.P.; Failla, S.; Di Bella, S. On the Aggregation and Sensing Properties of Zinc(II) Schiff-Base Complexes of Salen-Type Ligands. *Molecules* **2019**, *24*, 2514. [CrossRef] [PubMed]
32. Leoni, L.; Dalla Cort, A. The Supramolecular Attitude of Metal–Salophen and Metal–Salen Complexes. *Inorganics* **2018**, *6*, 42. [CrossRef]
33. Yin, H.-Y.; Tang, J.; Zhang, J.-L. Introducing Metallosalens into Biological Studies: The Renaissance of Traditional Coordination Complexes. *Eur. J. Inorg. Chem.* **2017**, *2017*, 5085–5093. [CrossRef]
34. Di Bella, S. Lewis acidic zinc(II) salen-type Schiff-base complexes: Sensing properties and responsive nanostructures. *Dalton Trans.* **2021**, *50*, 6050–6063. [CrossRef]
35. Consiglio, G.; Failla, S.; Finocchiaro, P.; Oliveri, I.P.; Purrello, R.; Di Bella, S. Supramolecular Aggregation/Deaggregation in Amphiphilic Dipolar Schiff-Base Zinc(II) Complexes. *Inorg. Chem.* **2010**, *49*, 5134–5142. [CrossRef] [PubMed]
36. Oliveri, I.P.; Di Bella, S.; Failla, S.; Malandrino, G. New molecular architectures by aggregation of tailored zinc(II) Schiff-base complexes. *New J. Chem.* **2011**, *35*, 2826–2831. [CrossRef]
37. Oliveri, I.P.; Di Bella, S. Sensitive Fluorescent Detection and Lewis Basicity of Aliphatic Amines. *J. Phys. Chem. A* **2011**, *115*, 14325–14330. [CrossRef] [PubMed]
38. Oliveri, I.P.; Di Bella, S. Highly sensitive fluorescent probe for detection of alkaloids. *Tetrahedron* **2011**, *67*, 9446–9449. [CrossRef]
39. Oliveri, I.P.; Di Bella, S. Lewis basicity of relevant monoanions in a non-protogenic organic solvent using a zinc(II) Schiff-base complex as a reference Lewis acid. *Dalton Trans.* **2017**, *46*, 11608–11614. [CrossRef]
40. Oliveri, I.P.; Malandrino, G.; Di Bella, S. Phase Transition and Vapochromism in Molecular Assemblies of a Polymorphic Zinc(II) Schiff-Base Complex. *Inorg. Chem.* **2014**, *53*, 9771–9777. [CrossRef]

41. Mirabella, S.; Oliveri, I.P.; Ruffino, F.; Maccarrone, G.; Di Bella, S. Low-cost chemiresistive sensor for volatile amines based on a 2D network of a zinc(II) Schiff-base complex. *Appl. Phys. Lett.* **2016**, *109*, 143108. [CrossRef]
42. Tang, J.; Cai, Y.-B.; Jing, J.; Zhang, J.-L. Unravelling the correlation between metal induced aggregation and cellular uptake/subcellular localization of Znsalen: An overlooked rule for design of luminescent metal probes. *Chem. Sci.* **2015**, *6*, 2389–2397. [CrossRef] [PubMed]
43. Tang, J.; Xie, D.; Yin, H.-Y.; Jing, J.; Zhang, J.-L. Cationic sulfonium functionalization renders Znsalens with high fluorescence, good water solubility and tunable cell-permeability. *Org. Biomol. Chem.* **2016**, *14*, 3360–3368. [CrossRef]
44. Strianese, M.; Guarnieri, D.; Lamberti, M.; Landi, A.; Peluso, A.; Pellecchia, C. Fluorescent salen-type Zn(II) Complexes As Probes for Detecting Hydrogen Sulfide and Its Anion: Bioimaging Applications. *Inorg. Chem.* **2020**, *59*, 15977–15986. [CrossRef]
45. Consiglio, G.; Oliveri, I.P.; Cacciola, S.; Maccarrone, G.; Failla, S.; Di Bella, S. Dinuclear zinc(II) salen-type Schiff-base complexes as molecular tweezers. *Dalton Trans.* **2020**, *49*, 5121–5133. [CrossRef]
46. Munzi, G.; Failla, S.; Di Bella, S. Highly selective and sensitive colorimetric/fluorometric dual mode detection of relevant biogenic amines. *Analyst* **2021**, *146*, 2144–2151. [CrossRef] [PubMed]
47. Oliveri, I.P.; Maccarrone, G.; Di Bella, S. A Lewis Basicity Scale in Dichloromethane for Amines and Common Nonprotogenic Solvents Using a Zinc(II) Schiff-Base Complex as Reference Lewis Acid. *J. Org. Chem.* **2011**, *76*, 8879–8884. [CrossRef]
48. Forte, G.; Oliveri, I.P.; Consiglio, G.; Failla, S.; Di Bella, S. On the Lewis acidic character of bis(salicylaldiminato)zinc(II) Schiff-base complexes: A computational and experimental investigation on a series of compounds varying the bridging diimine. *Dalton Trans.* **2017**, *46*, 4571–4581. [CrossRef]
49. She, N.; Moncelet, D.; Gilberg, L.; Lu, X.; Sindelar, V.; Briken, V.; Isaacs, L. Glycoluril-Derived Molecular Clips are Potent and Selective Receptors for Cationic Dyes in Water. *Chem. A Eur. J.* **2016**, *22*, 15270–15279. [CrossRef] [PubMed]
50. Burnett, C.A.; Witt, D.; Fettinger, J.C.; Isaacs, L. Acyclic Congener of Cucurbituril: Synthesis and Recognition Properties. *J. Org. Chem.* **2003**, *68*, 6184–6191. [CrossRef]
51. Heilmann, M.; Tiefenbacher, K. A Modular Phosphorylated Glycoluril-Derived Molecular Tweezer for Potent Binding of Aliphatic Diamines. *Chem. A Eur. J.* **2019**, *25*, 12900–12904. [CrossRef]
52. Solladié, N.; Aziat, F.; Bouatra, S.; Rein, R. Bis-porphyrin tweezers: Rigid or flexible linkers for better adjustment of the cavity to bidentate bases of various size. *J. Porphyr. Phthalocyanines* **2008**, *12*, 1250–1260. [CrossRef]
53. Murphy, R.B.; Pham, D.-T.; White, J.M.; Lincoln, S.F.; Johnston, M.R. Molecular tweezers with a rotationally restricted linker and freely rotating porphyrin moieties. *Org. Biomol. Chem.* **2018**, *16*, 6206–6223. [CrossRef] [PubMed]
54. Ballester, P.; Costa, A.; Castilla, A.M.; Deyà, P.M.; Frontera, A.; Gomila, R.M.; Hunter, C.A.; Costa, A. DABCO-Directed Self-Assembly of Bisporphyrins (DABCO=1,4-Diazabicyclo[2.2.2]octane). *Chem. A Eur. J.* **2005**, *11*, 2196–2206. [CrossRef]
55. Martin, R. Modes of action of anthelmintic drugs. *Veter. J.* **1997**, *154*, 11–34. [CrossRef]
56. Feron, P.H.M.; Cousins, A.; Jiang, K.; Zhai, R.; Garcia, M. An update of the benchmark post-combustion CO_2-capture technology. *Fuel* **2020**, *273*, 117776. [CrossRef]
57. Mazari, S.; Ali, B.S.; Jan, B.M.; Saeed, I.M. Degradation study of piperazine, its blends and structural analogs for CO_2 capture: A review. *Int. J. Greenh. Gas Control.* **2014**, *31*, 214–228. [CrossRef]
58. Kumar, R.R.; Sahu, B.; Pathania, S.; Singh, P.K.; Akhtar, M.J.; Kumar, B. Piperazine, a Key Substructure for Antidepressants: Its Role in Developments and Structure-Activity Relationships. *ChemMedChem* **2021**. [CrossRef]
59. Katz, D.P.; Deruiter, J.; Bhattacharya, D.; Ahuja, M.; Bhattacharya, S.; Clark, C.; Suppiramaniam, V.; Dhanasekaran, M. Benzylpiperazine: "A messy drug". *Drug Alcohol Depend.* **2016**, *164*, 1–7. [CrossRef] [PubMed]
60. Nguyen, H.L.; Yiannias, J.A. Contact Dermatitis to Medications and Skin Products. *Clin. Rev. Allergy Immunol.* **2018**, *56*, 41–59. [CrossRef]
61. Eide-Haugmo, I.; Brakstad, O.G.; Hoff, K.A.; Sørheim, K.R.; da Silva, E.F.; Svendsen, H.F. Environmental impact of amines. *Energy Procedia* **2009**, *1*, 1297–1304. [CrossRef]
62. European Chemicals Bureau; Institute for Health and Consumer Protection E.U. Risk Assessment Report-Piperazine; Munn, S.J.; Allanou, R.; Aschberger, K.; Cosgrove, O.; Pakalin, S.; Paya-Perez, A.; Pellegrini, G.; Schwarz-Schulz, B.; et al. Office for Official Publications of the European Communities, Luxemburg. 2005. Available online: https://echa.europa.eu/documents/10162/35f9602c-cb84-448f-9383-250e1a5ad350 (accessed on 11 April 2021).
63. El-Shabouri, S.R.; Mohamed, F.A.; Mohamed, A.M.I. A rapid spectrophotometric method for determination of piperazine. *Talanta* **1987**, *34*, 968–970. [CrossRef]
64. Wahbi, A.-A.M.; Abounassif, M.A.; Gad-Kariem, E.A. Colorimetric determination of piperazine with p-benzoquinone. *Talanta* **1986**, *33*, 179–181. [CrossRef]
65. Wahbi, A.-A.M.; Abounassif, M.; Kariem, E.A. Spectrophometric determination of piperazine with chloranil. *Analyst* **1984**, *109*, 1513–1514. [CrossRef]
66. Muralikrishna, U.; Krishnamurthy, M.; Rao, N.S. Analytical uses of charge-transfer complexes: Determination of pure and dosage forms of piperazine. *Analyst* **1984**, *109*, 1277–1279. [CrossRef]
67. Bu, X.; Pang, M.; Wang, B.; Zhang, Y.; Xie, K.; Zhao, X.; Wang, Y.; Guo, Y.; Liu, C.; Wang, R.; et al. Determination of Piperazine in Eggs Using Accelerated Solvent Extraction (ASE) and Solid Phase Extraction (SPE) with High-Performance Liquid Chromatography—Fluorescence Detection (HPLC-FLD) and Pre-Column Derivatization with Dansyl Chloride. *Anal. Lett.* **2019**, *53*, 53–71. [CrossRef]

68. Hadi, M.; Ahmadvand, E.; Ehsani, A. Electroanalytical Sensing of Piperazine at Carbon Nanotubes/Nafion Composite-modified Glassy Carbon and Screen-printed Carbon Electrodes in Human Plasma. *J. Anal. Chem.* **2020**, *75*, 238–245. [CrossRef]
69. Denis, C.M.; Baryla, N.E. Determination of piperazine in pharmaceutical drug substances using capillary electrophoresis with indirect UV detection. *J. Chromatogr. A* **2006**, *1110*, 268–271. [CrossRef] [PubMed]
70. Guanais Goncalves, C.; Dini, F.; Martinelli, E.; Catini, A.; Lundström, I.; Paolesse, R.; Di Natale, C. Detection of diverse potential threats in water with an array of optical sensors. *Sens. Actuators B Chem.* **2016**, *236*, 997–1004. [CrossRef]
71. Lu, G.; Grossman, J.E.; Lambert, J.B. General but Discriminating Fluorescent Chemosensor for Aliphatic Amines. *J. Org. Chem.* **2006**, *71*, 1769–1776. [CrossRef]
72. McGrier, P.L.; Solntsev, K.M.; Miao, S.; Tolbert, L.M.; Miranda, O.R.; Rotello, V.M.; Bunz, U.H.F. Hydroxycruciforms: Amine-Responsive Fluorophores. *Chem. A Eur. J.* **2008**, *14*, 4503–4510. [CrossRef]
73. Thordarson, P. Determining association constants from titration experiments in supramolecular chemistry. *Chem. Soc. Rev.* **2010**, *40*, 1305–1323. [CrossRef] [PubMed]
74. Bourson, J.; Pouget, J.; Valeur, B. Ion-responsive fluorescent compounds. 4. Effect of cation binding on the photophysical properties of a coumarin linked to monoaza- and diaza-crown ethers. *J. Phys. Chem.* **1993**, *97*, 4552–4557. [CrossRef]
75. Currie, L.A. Detection and quantification limits: Origins and historical overview. *Anal. Chim. Acta* **1999**, *391*, 127–134. [CrossRef]
76. Analytical Methods Committee, Recommendations for the definition, estimation and use of the detection limit. *Analyst* **1987**, *112*, 199–204. [CrossRef]